Overview of Commissioning Operations on the National Spherical Torus Experiment Upgrade (NSTX-U)

D.J. Battaglia[1], F. Bedoya[2], R.E. Bell[1], J.W. Berkery[3], M.D. Boyer[1], A. Diallo[1], E. Fredrickson[1], S. Gerhardt[1], W. Guttenfelder[1], M. Jaworski[1], S.M. Kaye[1], B.P. LeBlanc[1], R. Perkins[1], M. Podesta[1], R. Maingi[1], D. Mueller[1], J.E. Menard[1], C.E. Myers[1], M. Ono[1], R. Raman[4], S.A. Sabbagh[3], F. Scotti[5], V. Soukhanovskii[5], the NSTX-U Research Team

[1] *Princeton Plasma Physics Laboratory, Princeton, New Jersey, USA*

[2] *University of Illinois at Urbana – Champaign, Champaign, Illinois, USA*

[3] *Columbia University, New York, New York, USA*

[4] *University of Washington, Seattle, Washington, USA*

[5] *Lawrence Livermore National Laboratory, Livermore, California, USA*

The first plasma discharge of the National Spherical Torus Experiment Upgrade (NSTX-U) was produced on August 10, 2015 at the Princeton Plasma Physics Laboratory (PPPL) in Princeton, NJ. The inaugural discharge marked the completion of a multi-year upgrade of the NSTX experiment aimed at extending the performance of magnetic confinement of high-temperature plasmas in a low-aspect ratio toroidal geometry [1,2,3]. NSTX-U will advance the physics basis required for achieving steady-state, high-beta, and high-confinement conditions in a tokamak by accessing high toroidal field (B_{T0} = 1 T) and plasma current (I_p = 1.0 – 2.0 MA) in a low-aspect-ratio geometry (A = 1.6 – 1.8) with flexible auxiliary heating systems (P_{NBI} = 12 MW, P_{RF} = 2 MW). The new performance regimes are enabled by the recent modifications to NSTX, primarily the replacement of the center stack (i.e. the ohmic solenoid and inner TF legs) and the addition of three neutral beam sources that have more tangential injection angles than the three original beams on NSTX. The initial ten weeks of operation on NSTX-U constituted the commissioning phase, which focused on qualifying the tools and scenarios required for the first experimental campaign. About 90% of the commissioning activities were competed before the campaign was terminated prematurely due to the failure of a poloidal field coil.

The new ohmic solenoid provides a factor-of-three increase in the ohmic flux available to inductively sustain the plasma current. This new capability extended the length of the L-mode discharges such that the maximum pulse length (2 s) with I_p = 0.65 MA and B_T = 0.65 T simultaneously exceeded the longest discharges and the largest on-axis B_T (0.55T) from NSTX operations. The long-pulse stationary L-mode discharges with regular sawtooth activity are novel for spherical tokamaks and support initial experiments in error field identification and correction, core and SOL transport and fast-ion physics during the commissioning campaign. Figure 1 compares two 1 MA L-mode discharges (blue and red) to an H-mode discharge (black) on NSTX-U. Discharge 203582 (blue traces) operates with 1MW of NBI heating at lower density, while discharge 204556 (red traces) supports about 3 MW at higher density. Both discharges operate slightly below the L-H power threshold in a shape biased LSN (red trace in figure 1k) that is the favorable ion grad-B drift direction. The

internal inductance (figure 1c) is above 1.0 in L-mode, limiting the elongation (figure 1d) to values below 2 in order to maintain vertical stablity. The low elongation in L-mode discharges restricts the triangularity to a modest value ($\delta \sim 0.35$) with the outboard strikepoint on the outer divertor target ($R \sim 1$ m). These stationary L-mode discharges provide a connection to standard-aspect ratio regimes that achieve L-mode confinement ($H_{98y,2} \sim 0.5$) at modest β ($\beta_N \leq 2$) for probing the aspect ratio dependence of transport and stability physics [4].

Active feedback of the plasma shape was first achieved using feedback on the radial gaps between the outboard plasma boundary and the wall and feed-forward divertor coil currents. Within a few weeks of operation, active shape control of the plasma boundary and X-point locations using real-time equilibrium reconstructions (rtEFIT) was commissioned including multiple-in-multiple-out (MIMO) controls of the inner gap and X-point or strike point locations. The plasma control system (PCS) for NSTX-U underwent significant revisions during the upgrade period, including the restructuring of the control algorithms into a "state-machine" architecture. This modification supports future disruption avoidance and mitigation studies, where the active control algorithms are dependent on the state of the discharge. This architecture was used during the commissioning phase to initiate controlled terminations of discharges when a loss-of-control event occurred, including loss of vertical control and the ohmic solenoid approaching a current or heating limit.

High-performance H-mode scenarios on NSTX-U are projected to require vertical stabilization at high elongation ($\kappa > 2.5$) and high triangularity ($\delta \sim 0.7$) [1,2]. These highly-

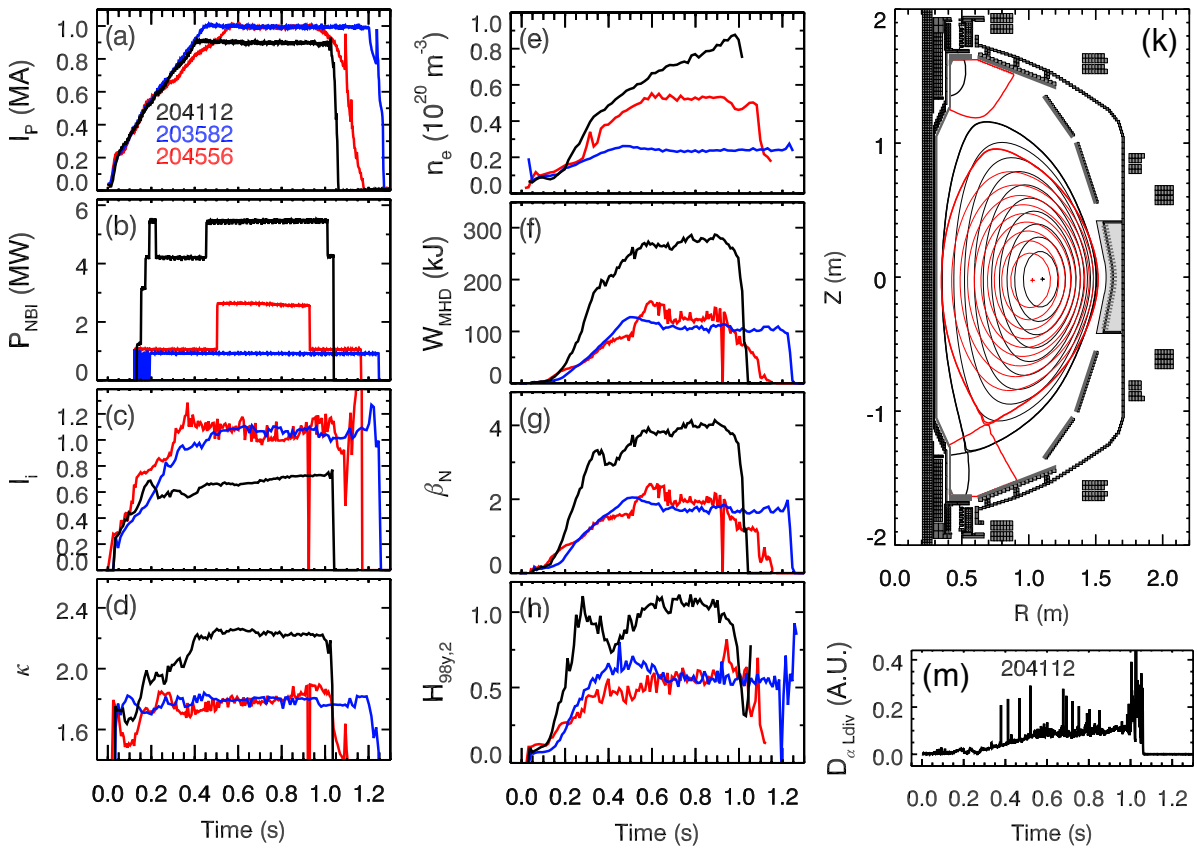

Figure 1 H-mode (black) and L-mode (blue and red) discharges from the commissioning phase of NSTX-U. (a) Plasma current, (b) neutral beam heating power, (c) internal inductance, (d) elongation, (e) line-averaged electron density, (f) stored energy, (g) normalized β and (h) confinement scaling factor are shown versus time. (k) Characteristic magnetic equilibrium for the H-mode discharge and one of the L-mode discharges, both at 0.8s. (m) D_α filterscope signal viewing the lower divertor for the H-mode shot

shaped discharges were realized on NSTX, albeit at lower aspect ratio. The requirement for routine operation at high elongation motivated improvements in the vertical motion detection on NSTX-U, including increasing the poloidal sensor pairs from one to nine and using real-time signal processing to remove spurious spikes in the calculated motion from the pick-up of power supply switching noise on magnetic sensors. These improvements allowed for the stable operation of $\kappa = 2.4$ at $l_i > 0.7$ similar to the performance realized on NSTX.

Long-pulse beam-heated L-mode discharges were used to investigate the source of error fields and optimum error field correction (EFC) scheme using six window-frame coils (i.e. RWM coils) on the outboard midplane of NSTX-U. A series of "compass scans" were completed whereby the amplitude of an applied n=1 field from the RWM coils was increased at various toroidal phases to identify the critical amplitude for triggering a locked mode. The results of these scans, combined with coil metrology and resistive and ideal MHD calculations indicated that a static misalignment of the inner legs of the TF in respect to the poloidal field coil planes was the largest source of an n = 1 error field. One feature of this error field source is the optimum EFC phase depends on the existence of low-order rational q surfaces, and thus the optimum EFC phase changed throughout I_p ramp-up. Future operations on NSTX-U aim to improve the alignment of the inner TF legs to minimize this error field source.

Steady progress in the wall conditions, real-time axisymmetric shape control, the availability of neutral beam heating and the correction of error fields led to increasing performance of the H-mode scenario during the commissioning phase. A number of discharges produced near the conclusion of the ten-week period satisfied the commissioning goal of producing H-mode discharges with regular ELMs and little core MHD activity to facilitate transport and stability studies. The black traces in figure 1 shows an example discharge (204112) with $I_p = 0.9$ MA and $P_{NBI} = 5.2$ MW. The L-H transition occurs at 0.2s during a transient pulse of NBI heating. The resulting increase in the plasma temperature and growth of the edge bootstrap current maintains the internal inductance (figure 1c) below 0.8 for the duration of the discharge. Thus, the discharge is vertically stable for $\kappa > 2$ (the limit to κ for $l_i < 0.8$ was, unfortunately, not established during this campaign). The elongation is suitable for achieving a highly shaped plasma boundary with $\delta \sim 0.65$ and biased LSN.

The discharge is free of core MHD prior to 1.0s with $\beta_N/\beta_{no\text{-}wall} \geq 1$ [5], $H_{98y,2} \geq 1$, and $\beta_N/l_i \sim 5.8$. The maximum ratio of β_N/l_i permitting MHD-free operations was found to improve with each successive improvement in error field correction during the course of the campaign. The ELMs are small (type III) or "grassy" (type V) as seen in the D_α signals from the lower divertor (figure 1m), until about 0.9s. The electron density (figure 1e) tends to rise faster during the ELM-free and grassy-ELM phases and approaches the Greenwald density limit at 1.0s. Spectroscopic data suggests the density rise is accompanied by an increase in the impurity content of the plasma, most likely reducing the net heating power available to sustain H-mode. The discharge ends with an H-L back transition that occurs shortly after the appearance of a core MHD mode around 1.0s. Future efforts to improve the wall conditioning, employ larger NBI heating and develop an optimized ramp-up scenario will aid in extending the length of the discharge, realizing stationary H-mode conditions and establishing a plasma shape with $\kappa > 2.5$.

Much of the progress in the commissioning phase was enabled by excellent availability of the plasma diagnostics. Within the first two weeks of operation, NSTX-U was

producing H-mode discharges with between-shot equilibrium calculations constrained by Thomson scattering measurements of the electron density and temperature. Operations relied heavily on the fast camera and filterscope systems that were operational from first plasma. A number of new diagnostics that supported the first experiments on NSTX-U were commissioned, including the real-time velocity (RTV) CHERS diagnostics [6] that provided high temporal measurements of the plasma rotation used to identify the phase of error fields while applying a rotating nonaxisymmetric field. In the future, this diagnostic will supply the fast plasma rotation and ion temperature measurements required for real-time feedback control of the plasma rotation and improved constraints within the real-time equilibrium reconstruction. A novel diagnostic for monitoring the first-wall chemistry, called the materials analysis and particle probe (MAPP) [7], provided valuable insight into the state of the wall conditions during the commissioning campaign. MAPP has the unique capability of exposing sample probes within the NSTX-U vacuum chamber during plasma operations and then completing surface analysis within a vacuum chamber attached to NSTX-U. This system provided day-to-day tracking of the first-wall surface chemistry and, in the future, will be capable of performing analysis following each plasma discharge.

NSTX-U had a productive commissioning period and is poised to quickly address key scientific issues when operations resume [8]. Initial experiments with the new, more tangential neutral beam lines demonstrated that these heating sources have a profound impact on the MHD stability through modification of the current and rotation profile; future experiments will employ these sources to actively control the kinetic profiles to study and optimize the stability in high-β regimes. Furthermore, injection from the new neutral beam lines was found to stabilize counter-propagating Global Alfven Eigenmodes (GAE) by adding a population of high pitch-angle beam ions [9]. The ability to suppress fast-ion modes through careful tailoring of the fast-ion distribution provides a mechanism for improving the energy confinement in NSTX-U and future burning plasmas, such as ITER.

A number of activities are being pursued in parallel with the repair of the failed poloidal field coil to enable operations at full field (B_T = 1 T, I_p = 2 MA) with an expanded diagnostic set. Access to this new regime at low-aspect-ratio will expand the physics basis required for optimizing the aspect ratio of future burning plasma devices.

This work was supported primarily by the DOE under Contract Number DE-AC02-09CH11466.

[1] Menard, J. E. *et al*. *Nucl*. *Fusion* **52,** 083015(39) (2012).

[2] Gerhardt, S. P., Andre, R. & Menard, J. E. *Nucl*. *Fusion* **52,** 083020 (2012).

[3] Ono, M. *et al*. *Nucl*. *Fusion* **55,** 73007 (2015).

[4] Guttenfelder, W. *et al*. *Nucl*. *Fusion, submitted*

[5] Berkery, J.W. *et al. Phys. Plasmas* **24**, 056103 (2017)

[6] Podestà, M. & Bell, R. E. *Plasma Phys*. *Control*. *Fusion* **58,** 125016 (2016).

[7] Bedoya, F. *et al*. *Nucl*. *Mater*. *Energy*, *accepted* (2017).

[8] Menard, J.E. et al, *Nucl*. *Fusion, accepted* (2017)

[9] Fredrickson, E. eta l., PRL, accepted (2017)